The age, distance and extinction of open clusters NGC0663, NGC1039 and NGC6939

T Szwarcer

February 2024

Abstract

Photometric data was collected from images of open clusters NGC0663, NGC1039 and NGC6939. This data was used alongside parallax and proper motion data from the ESA Gaia satellite to exclude field stars from the observations. Colour-magnitude diagrams were generated for each cluster, and a best-fit isochrone was identified by eye, yielding age, distance modulus and extinction estimates. The results are as follows: NGC0663: age $= 25^{+0}_{-5}$ Myr, $(m-M)_0 = 12.3^{+0.2}_{-0.6}$, $E(B-V) = 0.73^{+0.10}_{-0.05}$; NGC1039: age $= 501^{+130}_{-190}$ Myr, $(m-M)_0 = 8.5^{+0.5}_{-0.2}$, $E(B-V) = 0.05^{+0.08}_{-0.05}$; NGC6939: age $= 1260^{+330}_{-0}$ Myr, $(m-M)_0 = 10.9^{+0.2}_{-0.2}$, $E(B-V) = 0.28^{+0.05}_{-0.10}$. These results agree moderately well with literature, although it is suspected $E(B-V)$ was systematically underestimated as our values were lower than those from literature in all cases.

1 Introduction

The study of star clusters is of great importance in astrophysics. Members of a cluster were formed at roughly the same time, i.e. when the parent molecular cloud collapsed. This allows for stellar isochrones (lines of constant age) to be fitted to observational colour-magnitude diagrams. From these, the age, distance and extinction (a measure of the scattering of light from the source due to interstellar gas and dust) of the clusters can be inferred. These parameters can be used to compare stellar evolution between clusters, in order to refine theoretical models of the stellar life-cycle.

This investigation focuses on open clusters: these lie in the plane of the galaxy and contain 10-1000 weakly bound members, typically dissociating within a few Gyr [1]. In this investigation, data from the Philip Wetton Telescope (PWT) was used in conjunction with proper motion and parallax data from the ESA Gaia satellite [2] to confirm star membership within the clusters NGC0663, NGC1039 and NGC6939. Confirmed members were then plotted on colour magnitude diagrams, with a best-fit isochrone yielding the aforementioned parameters of each.

2 Methodology

2.1 Data Reduction and Calibration

The PWT is a 40cm Meade LX200 Schmidt-Cassegrain telescope [3]. Raw images from the PWT were reduced using bias, dark and flat field frames. This calibration enabled accurate photometry to be done, which in turn allows for accurate software-based star detection from the images. The calibration frames from the observation of NGC0663 were reused in the reduction of observations of NGC1039 and NGC6939.

The conversion between counts per second (cps) as measured by the detector and the apparent magnitude of the object under observation carries a zero-point offset. A star finding chart was provided [1]. This was used to identify the measured cps value of three stars of known magnitude, from which the average zero-point could be found via the equation

$$m = \text{zero-point} - 2.5\log_{10}(\text{measured cps}) \tag{1}$$

where m is apparent magnitude. The data from the PWT was divided into B (blue) and V (visual) images following the Johnson-Morgan photometric system [4]. These filters correspond to images centered on the 440nm and 550nm regions of the spectrum respectively. Using the images of NGC0663,

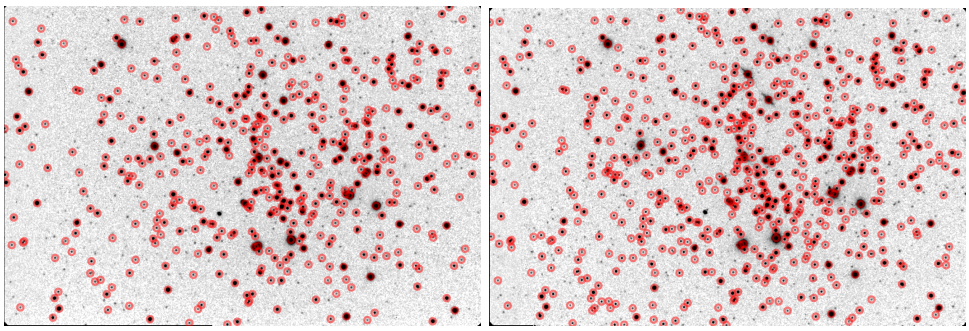

(a) B filter (b) V filter

Figure 1: Stars identified by the DAOFIND algorithm in both B and V filters for NGC0663.

the zero-point for both B and V filters was found. As the zero-point depends only on the detector used, and the PWT was used to capture all images, it was assumed not to vary between observations of the three clusters.

2.2 Star Identification and Photometry

The DAOFIND algorithm [5] was used to generate a list of star coordinates from the reduced images, as well as a visual illustration of the outcome (Figure 1). A measurement of full width, half-maximum (FWHM) of the imaged stars was obtained through analysis with the software QFitsView [6]. The FWHM was found by considering the number of pixels from the centre of an imaged star at which the cps value fell to half of its maximum. An aperture radius of $1.9 \times$ FWHM was used to compromise between collecting most of a star's flux and signal to noise ratio. This was used in a photometry program (using the Python Photutils package [7]) to generate a file containing star positions and corresponding magnitudes in the B and V filters.

2.3 Confirming Cluster Membership

As the PWT imaged many field stars (stars not in the cluster under consideration), additional processing was required to remove these from the dataset. The PWT images only contain star position and magnitude data, whereas the Gaia data includes proper motion and parallax values for each star. This can be used to confirm cluster membership.

2.3.1 Proper Motion

As the cluster members are gravitationally bound, they will have very similar proper motion. This can therefore be used as a criteria for membership. The software TOPCAT [8] was used to match

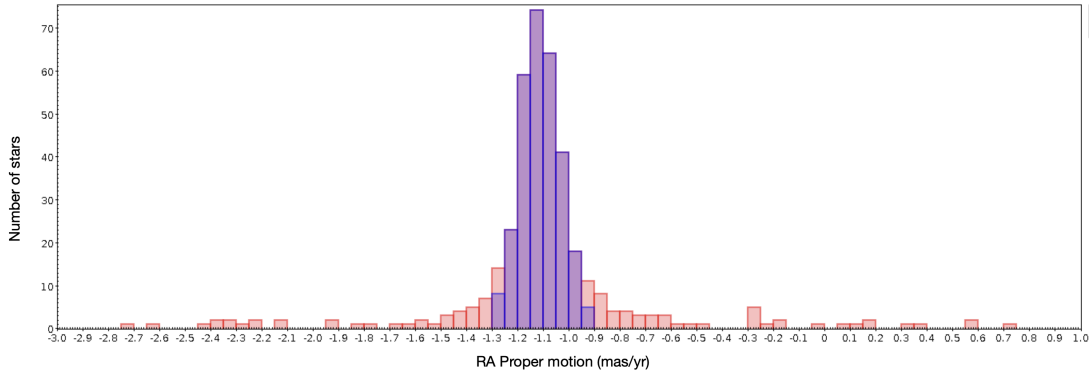

Figure 2: Histogram showing the distribution of proper motions in the RA direction for the image containing NGC0663. The first subset of likely members is shown in blue. This subset was refined further by repeating this process in the DE direction. Note the actual bin width is smaller than the 0.1mas/yr resolution of the chart.

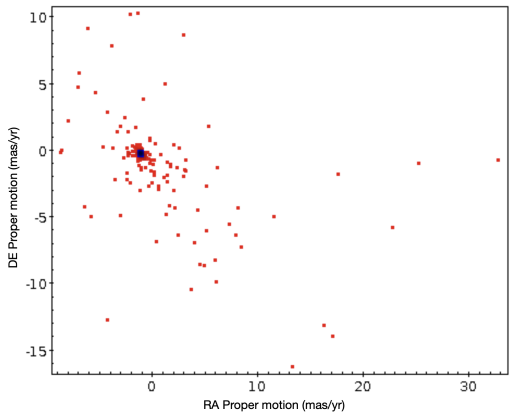

(a) Subset of likely NGC0663 members, shown in comparison to the whole set of imaged stars.

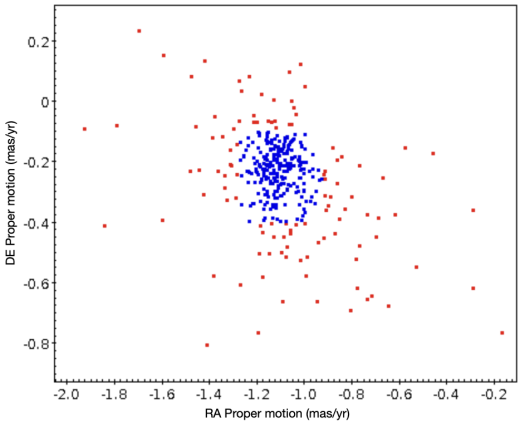

(b) As in 3a, showing only the region around the subset.

Figure 3: Plots of proper motion of stars in the NGC0663 image, showing the subset of likely members in blue.

stars from the Gaia data to the PWT data, by comparing star positions between the datasets and retaining those with positions matching within 1". Following this, a histogram of proper motion in each direction was generated. Stars with a proper motion within the approximate FWHM of the peak formed the first subset of cluster members. A visualisation of this process (for NGC0663) can be seen in Figures 2 and 3.

2.3.2 Parallax

When observing distant objects, the parallax angle will be on the order of the measurement resolution, and thus accurate conclusions cannot be drawn from such data. The clusters NGC1039 and NGC6939 are nearer to Earth than NGC0663: previous work gives $(m-M)_0 = 8.38$ [9], 11.0 [10] and 11.6 [11] respectively. Hence, in these cases parallax data can be more reliably used alongside proper motion data to further refine the subset of cluster members. Once the first subset of members had been created for these clusters, TOPCAT was used to generate a histogram of the parallaxes of the imaged stars. Stars with parallaxes approximately within the FWHM of the peak were selected as members. A visualisation of this process (for NGC1039) can be seen in Figure 4.

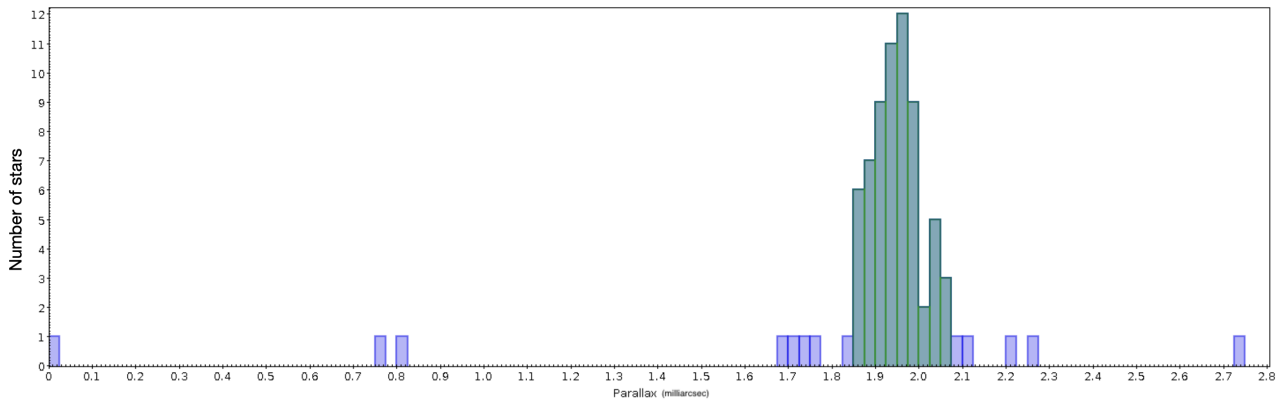

Figure 4: Histogram showing the distribution of parallaxes for the image containing NGC1039. The subset of likely members is shown in green.

2.4 Fitting The Stellar Isochrones

Once members of each cluster were identified, plots of V magnitude against B-V magnitude were generated. An isochrone was superimposed on the image and parameters adjusted until the best fit

was found, judged by eye. A fit was deemed acceptable if the isochrone roughly followed the trend of the data, with a similar number of data points falling either side of it.

3 Results

Table 1: Table showing the observed cluster parameters.

Cluster	Age (Myr)	$(m-M)_0$	$E(B-V)$
NGC0663	25^{+0}_{-5}	$12.3^{+0.2}_{-0.6}$	$0.73^{+0.10}_{-0.05}$
NGC1039	501^{+130}_{-190}	$8.5^{+0.5}_{-0.2}$	$0.05^{+0.08}_{-0.05}$
NGC6939	1260^{+330}_{-0}	$10.9^{+0.2}_{-0.2}$	$0.28^{+0.05}_{-0.10}$

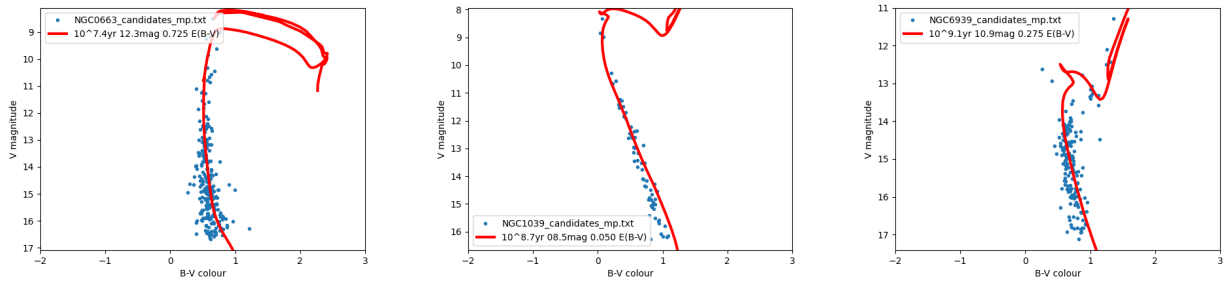

(a) NGC0663 (b) NGC1039 (c) NGC6939

Figure 5: Colour magnitude diagrams with best-fit isochrones for the three clusters.

3.1 Background

3.1.1 Isochrone Features

Isochrones for a given open cluster are in general parameterised by the cluster's age, distance, extinction and metallicity (abundance of elements heavier than H and He). This investigation used isochrones generated by PARSEC [12], assuming the metallicity of each cluster to be that of the Sun. In general, isochrones will show a main sequence region followed by a turn-off point into the subgiant and giant branches. The latter regions often have a complex shape, due to variations in luminosity from the onset of fusion of new elements through the stellar life cycle. A notable example of this would be the 'blue loop' executed when helium burning begins in the cores of stars with mass $3M_\odot < M < 9M_\odot$ [13].

3.1.2 Measure of Distance Used

It should be noted that distance was presented in our software as a true distance modulus, $(m-M)_0$. This is a logarithmic measure of distance that takes into account interstellar extinction, as opposed to the visual distance modulus $(m-M)_v = m - M$ which does not account for extinction effects. The apparent and absolute magnitudes are given by m and M respectively. The two measures are related by the formula

$$(m-M)_0 = (m-M)_v - 3.1E(B-V) \tag{2}$$

where $E(B-V)$ is the extinction. The distance d (in parsecs) can be found by the formula

$$(m-M)_0 = 5\log_{10}(d) - 5. \tag{3}$$

3.2 Isochrones and Colour Magnitude Diagrams

The colour magnitude diagrams with fitted isochrones for the three clusters are shown in Figure 5. It can be seen that cluster members in NGC0663 and NGC1039 are largely distributed before the red giant turn-off point, indicating a main-sequence population. There were some members of NGC6939 in the red giant branch, consistent with its greater age.

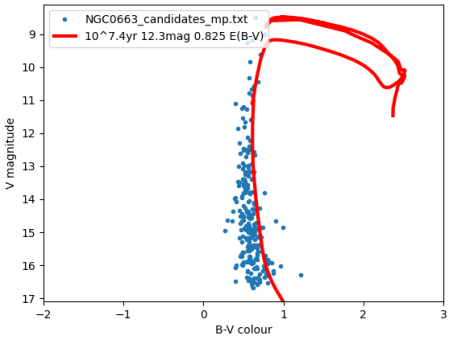

(a) Maximum extinction value (NGC0663)

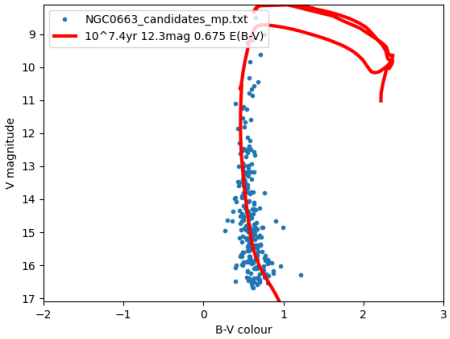

(b) Minimum extinction value (NGC0663)

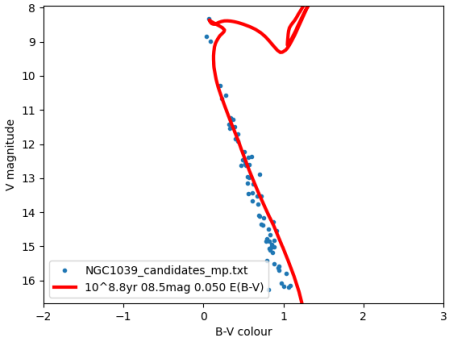

(c) Maximum age (NGC1039)

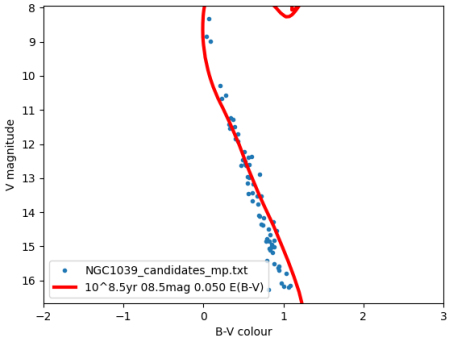

(d) Minimum age (NGC1039)

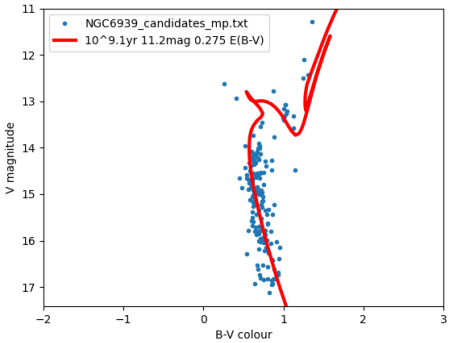

(e) Maximum distance modulus (NGC6939)

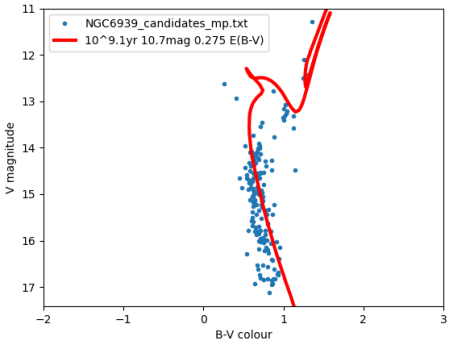

(f) Minimum distance modulus (NGC6939)

Figure 6: Examples of maximum and minimum parameters for the three clusters.

3.3 Consideration of Uncertainties

Any erroneous inclusion of field stars would have a negligible effect on the final parameters; the number of such stars is small compared to the number of correctly identified members, and thus would not affect the fit considering the criteria outlined in Section 2.4. Conclusions could not be drawn from errors in the photometric calculations as the isochrone fitting software used did not have the capacity to display error bars.

To quantify the uncertainty in the results, two parameters were fixed to their best-fit value and plots were produced varying the third to a maximum and minimum value such that the fit was at the limit of being acceptable. Examples of these are shown in Figure 6. Probable ranges for the parameters can be inferred from this, and thus uncertainties can be estimated. The set of final parameter estimates with uncertainties is presented in Table 1.

4 Analysis

4.1 Agreement with Literature

4.1.1 NGC0663

Table 2: Table showing parameters for NGC0663 taken from the literature.

Paper	Age (Myr)	$(m-M)_0$	E(B-V)
van den Bergh & de Roux 1978 [14]	-	11.55±0.04	0.8-1.0
Fabregat & Capilla 2005 [15]	25^{+7}_{-5}	11.6±0.1	-
Pigulski et al 2001 [11]	20-25	11.6	0.83
This paper	25^{+0}_{-5}	$12.3^{+0.2}_{-0.6}$	$0.73^{+0.10}_{-0.05}$

A summary of results from the literature is displayed in Table 2. We see excellent agreement in the age of the cluster. The observed extinction value is lower than typical values from the literature. If our value were an underestimate of the true value, we would expect a corresponding overestimation of distance modulus, which can be seen in Table 2 .

4.1.2 NGC1039

Table 3: Table showing parameters for NGC1039 taken from the literature.

Paper	Age (Myr)	$(m-M)_0$	E(B-V)
Jones & Prosser 1996 [9]	200-250	8.38	0.07
Ianna & Schlemmer 1993 [16]	250	8.28±0.09	-
Canterna et al 1979 [17]	500	8.2	0.07
This paper	501^{+130}_{-190}	$8.5^{+0.5}_{-0.2}$	$0.05^{+0.08}_{-0.05}$

A summary of results from the literature is displayed in Table 3. We see good agreement in the age of the cluster with Canterna et al. Both Jones & Prosser and Ianna & Schlemmer use a similar method of fitting theoretical isochrones to data, obtaining results that are consistent with each other, but not with ours. As there were few stars near the turn-off point in this cluster, there would have been some uncertainty in the position of this point, which would significantly impact the estimated age. The value for distance modulus is in good agreement with the literature, as is the extinction, although the latter has a large uncertainty so conclusions through comparisons to literature values should not be drawn.

4.1.3 NGC6939

Table 4: Table showing parameters for NGC6939 taken from the literature. An asterisk indicates where $(m-M)_v$ was reported, and converted to $(m-M)_0$.

Paper	Age (Myr)	$(m-M)_0$ (mag)	E(B-V) (mag)
Maciejewski & Niedzielski 2007 [10]	1260	11.0*	$0.38^{+0.18}_{-0.10}$
Rosvick & Balam 2002 [18]	1600±300	11.25*	0.33±0.07
Andreuzzi et al 2003 [19]	1000-1300	11.3-11.4	0.34-0.38
This paper	1260^{+330}_{-0}	$10.9^{+0.2}_{-0.2}$	$0.28^{+0.05}_{-0.10}$

It should be noted that two of the papers included here reported the visual distance modulus $(m-M)_v$ as opposed to the true distance modulus $(m-M)_0$ used in our fitting program. These values were converted to $(m-M)_0$ and presented in Table 4 for comparison with our measurements. We find excellent agreement in the age of the cluster and a good agreement in distance modulus. The

agreement of E(B-V) is less good; all measurements of E(B-V) have been below those found in the literature, so it may be possible the method used in this investigation systematically underestimates E(B-V).

4.2 Possible Improvements to Methodology

There were two main areas for improvement, both of which are alternatives to the more qualitative 'by-eye' approach taken in this investigation. Firstly, a least-squares process could have been used to more accurately determine the best-fit isochrone and corresponding parameters. Secondly, consideration of membership probabilities (e.g. Griggio & Beddin 2022 [20]) could have been used as a more quantitative membership criterion. When paired with the aforementioned fitting method, this would have allowed for accurate calculations of uncertainties in the fit.

It should be noted that better-fitting isochrones could in theory be obtained by treating metallicity as an additional free parameter; metallicity values could be found for each cluster through spectrophotometric analysis. Nevertheless, due to the limited resolution of the plotting software, and given that satisfactory fits could still be found for the solar case considered here, it is unlikely this would significantly change the results.

5 Conclusions

This paper presents the results of BV photometry on the open clusters NGC0663, NGC1039 and NGC6939. Results were in moderate agreement with the literature, likely hindered by the inaccurate 'by-eye' approach taken to confirming cluster membership and fitting stellar isochrones.

References

[1] University of Oxford. *Colour-magnitude diagrams of open clusters*. 2021.

[2] URL: `https://www.cosmos.esa.int/web/gaia/dr2`.

[3] URL: `http://observatory.physics.ox.ac.uk/about.php`.

[4] H L Johnson and W W Morgan. "Fundamental stellar photometry for standards of spectral type on the Revised System of the Yerkes Spectral Atlas". In: *Astrophysical Journal, Vol. 117, p. 313* (1953).

[5] P B Stetson. "DAOPHOT: A COMPUTER PROGRAM FOR CROWDED-FIELD STELLAR PHOTOMETRY". In: *Publications of the Astronomical Society of the Pacific, Vol 99* (1987).

[6] URL: `https://www.mpe.mpg.de/~ott/QFitsView/`.

[7] URL: `https://photutils.readthedocs.io/en/stable/`.

[8] URL: `https://www.star.bris.ac.uk/~mbt/topcat/`.

[9] B F Jones and C F Prosser. "Membership of stars in NGC 1039 (M34)". In: *Astronomical Journal v.111, p.1193* (1996).

[10] G Maciejewski and A Niedzielski. "CCD BV survey of 42 open clusters". In: *A&A vol. 467, 1065–1074* (2007).

[11] A Pigulski, G Kopacki, and Z Kolaczkowski. "The young open cluster NGC663 and its Be stars". In: *A&A, vol. 376, 144-153* (2001).

[12] A Bressan et al. "PARSEC: stellar tracks and isochrones with the PAdova and TRieste Stellar Evolution Code". In: *Monthly Notices of the Royal Astronomical Society, Volume 427, Issue 1* (2012).

[13] J J Walmswell, C A Tout, and J J Eldridge. "On the blue loops of intermediate-mass stars". In: *Monthly Notices of the Royal Astronomical Society, Volume 447, Issue 3* (2015).

[14] S van den Bergh and J de Roux. "UBV photometry of the open cluster NGC 663". In: *Astronomical Journal, v.83, p.1075* (1978).

[15] J Fabregat and G Capilla. "CCD *uvbyβ* photometry of the young open cluster NGC 663". In: *Monthly Notices of the Royal Astronomical Society, Volume 358, Issue 1, Pages 66–70* (2005).

[16] P A Ianna and D M Schlemmer. "Membership in the Galactic open cluster NGC 1039 (M34)". In: *Astronomical Journal (ISSN 0004-6256), vol. 105, no. 1, p. 209-219* (1993).

[17] R Canterna, C L Perry, and D L Crawford. "MULTICOLOR PHOTOMETRY OF THE GALACTIC CLUSTER NGC 1039 (M34)". In: *PASP **91** 263* (1979).

[18] J M Rosvick and D Balam. "CCD observations of the open cluster NGC6939". In: *The Astronomical Journal, 124:2093–2099* (2002).

[19] G Andreuzzi et al. "UBVI photometry of the intermediate-age open cluster NGC 6939". In: *Monthly Notices of the Royal Astronomical Society, Volume 348, Issue 1, Pages 297–306* (2004).

[20] M Griggio and L R Beddin. "Astrometric star-cluster membership probability: application to the case of M 37 with Gaia EDR3". In: *Monthly Notices of the Royal Astronomical Society, Volume 511, Issue 4, Pages 4702–4709* (2022).